Results in Physics 18 (2020) 103228

Contents lists available at ScienceDirect

Results in Physics

journal homepage: www.elsevier.com/locate/rinp

# Copper nanowires based mode-locker for soliton nanosecond pulse generation in erbium-doped fiber laser

E.I. Ismail[a], F. Ahmad[a], S. Shafie[b,d,*], H. Yahaya[a], A.A. Latif[c], F.D. Muhammad[c]

[a] Malaysia-Japan International Institute of Technology, Universiti Teknologi Malaysia, Jalan Sultan Yahya Petra, 54100 Kuala Lumpur, Malaysia
[b] Institute of Advanced Technology, Universiti Putra Malaysia, 43400 UPM Serdang, Selangor, Malaysia
[c] Department of Physics, Faculty of Science, Universiti Putra Malaysia, 43400 UPM Serdang, Selangor, Malaysia
[d] Department of Electrical and Electronic Engineering, Faculty of Engineering, Universiti Putra Malaysia, 43400 UPM Serdang, Selangor, Malaysia

ARTICLE INFO

*Keywords:*
Nanosecond pulse
Fiber laser
Copper nanowires

ABSTRACT

A mode-locked nanosecond Erbium-doped fiber laser (EDFL) based on copper nanowires (CuNWs) saturable absorber (SA) is successfully demonstrated in this article. The CuNWs were prepared by dissolving the CuNWs solution in a polydimethylsiloxane (PDMS) host polymer. Through the doctor blade technique, a free-standing CuNWs-PDMS film was formed. Upon inserting the film in a laser cavity, nanosecond pulses with a stable mode-locking was observed past the threshold pump power of 104.62 mW. The laser operated at the center frequency of 1.86 MHz and wavelength of 1563.3 nm. At the maximum available pump power of 187.04 mW, the 173 ns mode-locked pulse train achieved the highest pulse energy of 9.14 nJ and the maximum average output power of 1.703 mW. These results vindicate the capacity of the CuNWs film SA in producing nanosecond mode-locked EDFL in the 1550 nm region.

## Introduction

Due to numerous potential applications in the field of optoelectronics, electronics, and plasmonics [1], pulse lasers have continued to gain interests among researchers. For examples, passively mode-locked lasing in the 1.5-μm region have found many applications in telecommunication, material processing, and medical treatment. Generating pulse lasers using passive techniques require the use of saturable absorbers (SA). Passively generated lasers are favored due to their flexibility, simplicity, compactness, and ultrafast laser performance. The SAs can be fabricated from dyes/colored Glasses, semiconductor saturable absorber mirror (SESAM), quantum dots, 1D materials (carbon nanotubes), and 2D material (graphene, topological insulators (TIs), transition metal dichalcogenides (TMDs) and black phosphorous (BP) [2]. A good review on the use of 2D materials to construct passive saturable absorbers is available in [3]. However, 1-D and 2-D nanomaterials used for making SAs are expensive and thus research works exploring new SA materials are still active. Early works on finding and testing metal based nanomaterials for photonics applications can be traced back to the surface plasmon resonance applications. Recently, metal based nanomaterials have garnered increasing attention as excellent candidates for passive SA as they have a high intrinsic conductivity and are much cheaper compared to the cost of 1-D or 2-D nanomaterials.

It is our hope that the work explained in this article could expand the understanding on pulse laser generation using metal based nanomaterial saturable absorbers. Metal nanoparticles, including gold (Au), silver (Ag), and copper (Cu) possess strong absorption caused by the collective oscillation of conduction electrons of metal nanoparticles, namely as localized surface Plasmon resonance (LSPR). The strong resonance due to LSPR also contributes to the significant enhancement in optical nonlinearity, which is nonlinear absorption. Gold-based passive Q-switcher is reported in [4–6], and silver-based passive saturable absorber is reported in [7–9]. Compared to gold and silver, copper is more cost-effective and available in different forms. The lasers generated using copper-based passive saturable absorbers are reported to have operating frequencies covering from visible range to mid-infrared region with different starting materials such as copper pellets [10–12], copper nanoparticles [13,14], copper oxide nanopowder [15], and copper nanowires (CuNWs) [16].

Copper-based pellets have been deposited onto polyvinyl alcohol (PVA) film using an electron beam deposition method and used as passive saturable absorbers for pulsed laser generation in 1, 1.5 and 2 μm region [10–12]. In [10], the central wavelength for pulsed laser

* Corresponding author at: Department of Electrical and Electronic Engineering, Faculty of Engineering, Universiti Putra Malaysia, 43400 UPM Serdang, Selangor, Malaysia.
*E-mail address:* suhaidi@upm.edu.my (S. Shafie).

https://doi.org/10.1016/j.rinp.2020.103228
Received 13 February 2020; Received in revised form 30 June 2020; Accepted 3 July 2020
Available online 06 July 2020

generation was at 1040.6 nm with pulse repetition rates varying from 41 to 104 kHz. The shortest pulse width achieved was 3.89 μs, and the maximum pulse energy was 7.48 nJ with a signal to noise ratio of 57.6 dB. At 1.5 μm region [10,11], the reported pulsed fiber laser operated at 1561 nm with pulse energy of 18.34 nJ. The shortest pulse width was 4.28 μs, and signal to noise ratio was 50.9 dB. At 2 μm [12], the authors reported a mode-locked pulses operating at 1951 nm, with the fundamental frequency of 8.5 MHz. The calculated minimum pulse width was 14.8 ps and signal to noise ratio was 48 dB. In the work, the thickness of copper PVA film was 16 nm, but the size of the copper nanoparticles was not revealed. One of the drawbacks of this approach is the need for an evaporation chamber to evaporate the copper pellets.

Copper nanoparticle based powder with an average particle size of 25 nm was used as starting material to generate Q-switched pulsed in erbium-doped fiber laser [13,14]. Ismail et al. [13], reported copper nanoparticles in Chitosan-based passive saturable absorber. They reported a maximum repetition rate of 91.24 kHz, a minimum pulse width of 3.60 μs, and maximum pulse energy of 74.53 nJ. The generated pulse produces a signal to noise ratio (SNR) of 71 dB. Meanwhile, Ismail et al. [14] reported copper nanoparticles in polyvinyl alcohol (PVA) based passive saturable absorber. They reported the capability of a pulsed generation with a maximum repetition rate of 104.2 kHz, the narrowest pulse width of 5.1 μs, and pulse energy of 20.44 nJ at the maximum input pump power of 198.0 mW. The radio frequency spectrum analyzer measured the SNR of 54 dB. Even though the average particle size copper nanoparticles is 25 nm, the size could be affected during the ultrasonic process, and agglomeration occurs when the nanoparticles embedded in the host polymer. Copper oxide-based passive saturable absorber is reported in [15], where the copper oxide (CuO) nanopowder was dissolved in polyvinyl alcohol (PVA) to developed CuO-PVA film. The film then is integrated into an erbium-doped fiber laser to generate mode-locked pulsed at an operating wavelength of 1564.6 nm, a repetition rate of 983. kHz and signal to noise ratio of 24 dB. Unfortunately, the size of the copper nanopowder is not reported.

Wu et al. [16] reported a Q-switched pulse generation by using copper nanowires (Cu NWs) with a diameter of 20–40 nm as SA operating at a visible range laser region of 635 nm. To synthesize the CuNWs, a Copper (II) Chloride Dihydrate was added to glucose, oleymine, oleic acid, and ethanol before heated a 50 °C to produce CuNWs. The produced CuNWs is further refined through ultrasonication and centrifugation. To be used as a passive saturable absorber, the CuNWs suspension was further dispersed into polyvinyl alcohol (PVA) polymer and made into the polymer-composite structure. The CuNWs recorded an absorbance rate of 61.8% at 635 nm, yielding a Q-switched operation with a repetition rate ranging from 239.8 to 312.4 kHz, the pulse width of 0.685–0.394 μs and maximum output power up to 9.6 mW upon laser cavity integration, while no mode-locking operation was observed. The operation was relatively stable with an SNR of around 40 dB, attributed to the third-order nonlinearity of the CuNWs itself [16].

The pulse generation and advancement in lasers are dictated by two aspects, namely, nonlinearity and anomalous-dispersion balance which leads to the generation of ultrashort soliton mode-locked output [17]. The used of gain medium (EDF) can provide large normal dispersion, and the cavity dispersion can be managed to works in anomalous dispersion by adding a certain length of SMF in the laser cavity [18]. Certain value of anomalous dispersion should be achieved, because if the value is too small, the cavity will generate incoherent pulses. Several works had successfully demonstrated this approach to generate self-starting mode-locked for conventional soliton [18] and nanosecond pulse generation [19–22]. The length of the SMF to be added in the laser cavity depends on the respective anomalous dispersion requires by the laser cavity with the reported anomalous dispersion of $-4.23$ ps$^2$ [19], $-2.28$ ps$^2$ [20], $-4.30$ ps$^2$ [21], and 2.24 ps$^2$ [22] by using 100 m [20,22] and 195 m [19,21] of SMF.

In this works, we propose a mode-locked nanosecond Erbium-doped fiber laser (EDFL) based on copper nanowires in a polydimethylsiloxane (PDMS) polymer. By inserting the SA in a ring cavity and additional SMF of 100 m for dispersion management, nanosecond mode-locked pulses are generated with a repetition rate of 1.86 MHz, the pulse width of 173 ns, and signal to noise ratio of 61 dB, at the operating wavelength of 1563.3 nm.

## Fabrication and nonlinear characterization of CuNWs film

The commercial CuNWs used in this experiment was purchased from Sigma Aldrich®. The CuNWs solution was dispersed in ethanol with a concentration of 5 mg/mL. The diameter of the CuNWs is approximately 100 ± 20 nm with a length of 20–30 μm and aspect ratio of 200. The polymer composite Polydimethylsiloxane (PDMS) used in this work is the elastomer kit Sylgard 184 from Dow Corning Inc., consist of two components, siloxane oligomer, and hardener. In order to prepare the CuNWs/PDMS composite, 5 mL of CuNW solution was added into 10 mL of PDMS monomer and mixed together using a magnetic stirrer for 10 min at 1000 rpm. Then, 1 mL of hardener was added into CuNWs/PDMS monomer and stirred for another 10 min. The mixture of CuNWs/PDMS was then kept in the refrigerator overnight to remove any bubbles formed in the solution. The CuNWs/PDMS film was prepared using the doctor blade technique to develop a free-standing film. This method is widely used for producing thin films on large surface areas and accepted for precision coating methods [23]. In this technique, adhesive 3 M Scotch tape with a thickness of around 52 μm was placed on the edge of a glass substrate to create a 1 cm × 3 cm rectangular area for CuNWs/PDMS mixture deposition. Then, the CuNWs/PDMS was applied on the masked top edge of the glass substrate, and the mixture was spread homogenously across the unmasked area using a microscope glass slide. The scotch tape was then removed before having the CuNWs/PDMS solution thermally cured at 90 °C for 2 h. The CuNWs/PDMS film formation was finally detached from the glass slide to obtain a flexible and self-standing film, as shown in Fig. 1. This approach is convenient and straightforward for fiber compatibility

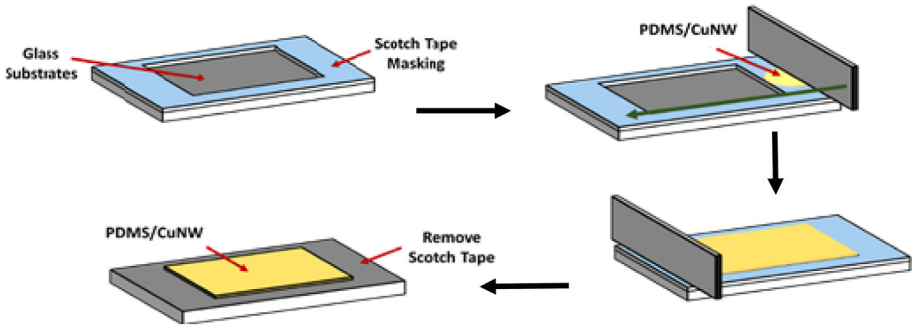


**Fig. 1.** The fabrication of the CuNW/PDMS film through Doctor Blade technique.

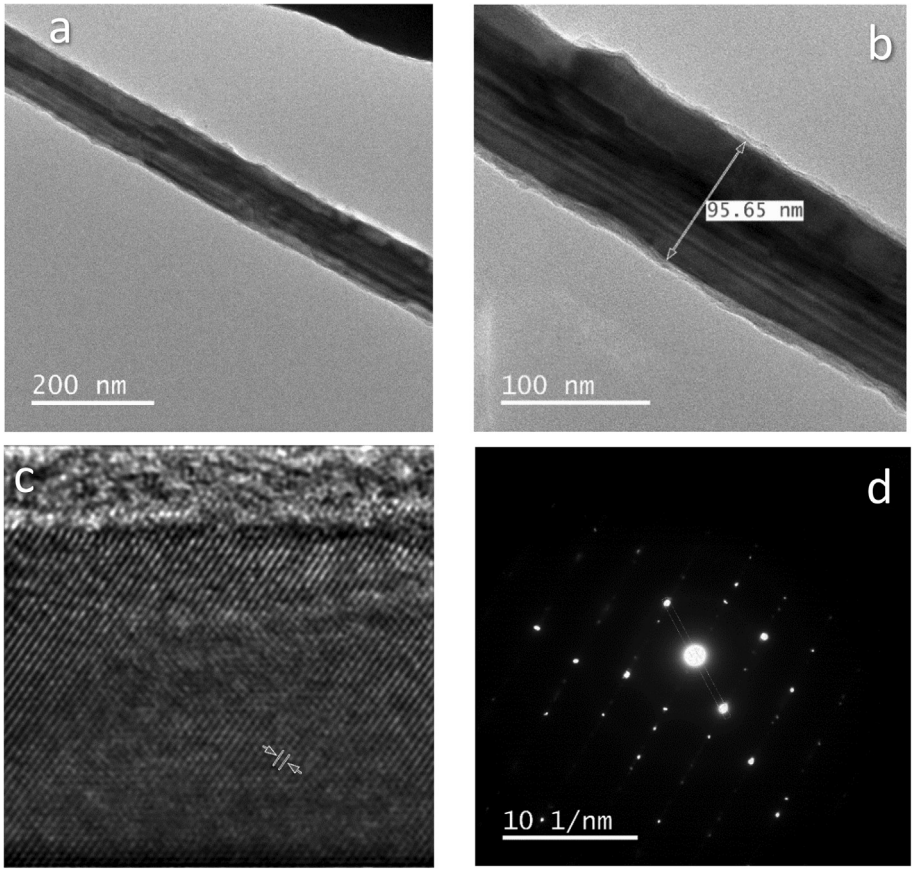


**Fig. 2.** transmission electron microscope (TEM) image of the CuNWs (a) TEM images of CuNWs at a magnification of x20k (b) HRTEM image of CuNWs at a magnification of x50k (c) HRTEM image of a CuNW at a magnification of x1000k. The lattice spacing was observed to be 0.24 nm. (d) TEM diffraction pattern of CuNW.

and creates a high oxidation resistance. The high oxidation resistance of the CuNWs/PDMS SA has also been reported by using spray coating and photonic sintering method [24].

Fig. 2 shows the transmission electron microscope (TEM) image of the CuNWs, which was measured by a high-resolution transmission electron microscope (HR-TEM) (JEOL, JEM-2100F). Fig. 2(a) and 2(b) show the TEM images of CuNWs with a diameter of about 95 nm. We can also observe the smooth surface of the CuNWs. Fig. 2(c) shows the measured lattice spacing of the CuNWs of approximately 0.24 nm, consistent with the one reported in by Wu et al., [16]. Fig. 2(d) shows the TEM diffraction pattern of CuNWs.

The field emission scanning electron microscope (FESEM) (JEOL JSM-7800F) image of the CuNWs/PDMS film is as depicted in Fig. 3. The accelerating voltage was set at 1 kV at the magnification of x7000 at the scale of one micron. The image shows irregular dispersion and sizes with a diameter of 100 nm to 2 um of the CuNWs throughout the film surface. This is due to phase separation in the evaporating solvent (hardener) during film formation. It is hard to get a better image at a higher magnification or higher kV (more than 1 kV) due to the sensitive nature of the PDMS monomer as the electron beam can cause the PDMS to melt.

The investigation of the nonlinear optical transmission property of the CuNWs/PDMS film is illustrated in Fig. 4. The nonlinear optical transmission profile of the prepared CuNWs-based SA film was investigated by using a balanced twin detector measurement with a mode-locked seed of 1 MHz repetition rate and 4.13 ps pulse width operating at 1550 nm wavelength. The modulation depth was around 8%, with a saturation intensity of 76.5 MW/cm$^2$. Besides that, we also examined the optical transmission range of the prepared CuNWs/PDMS based SA from 1100 nm to 1600 nm, as shown in Fig. 5, after it was illuminated by a broadband light source (AQ-4303B White Light Source). The absorption of the prepared CuNWs based SA can clearly be

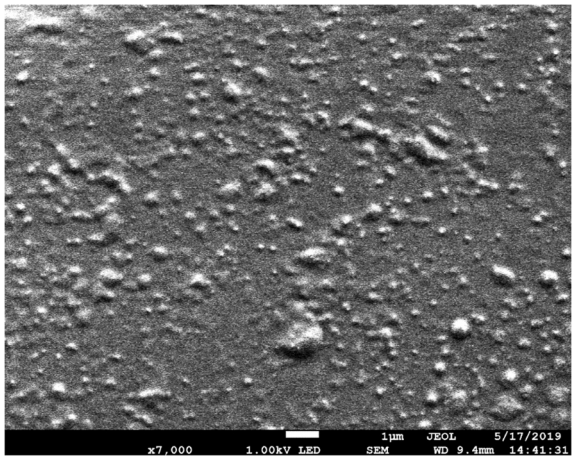


**Fig. 3.** Surface morphology of Copper Nanowires-PDMS.

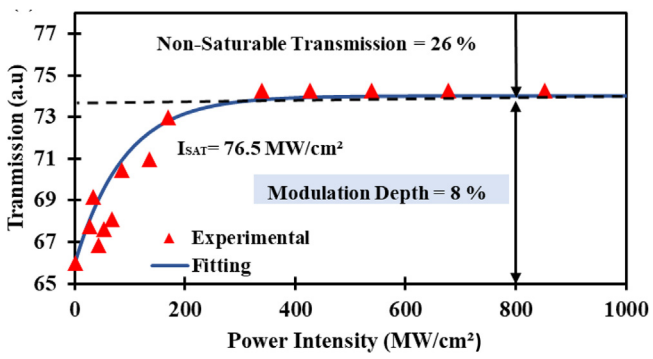


**Fig. 4.** Nonlinear transmission measurement of CuNWs/PDMS film.

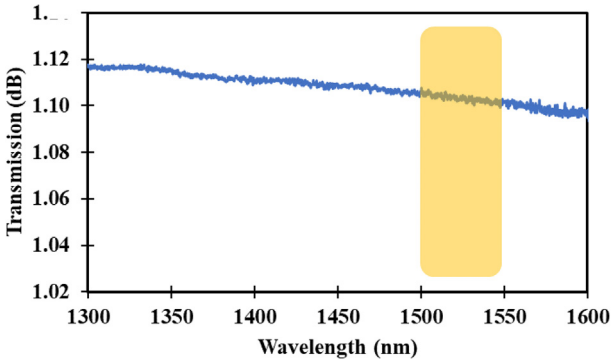


**Fig. 5.** Absorption spectrum of CuNWs/PDMS film with highlighted at C-band region.

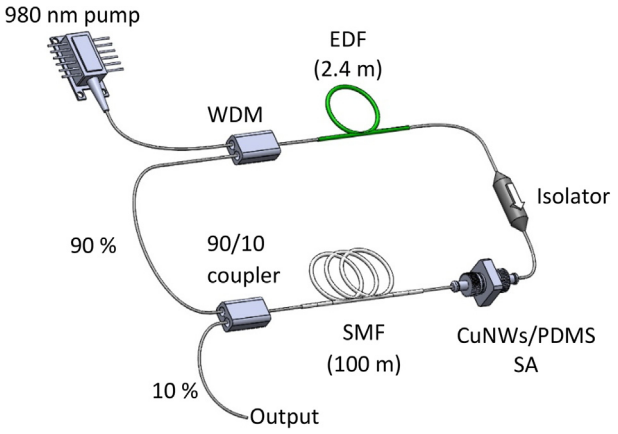


**Fig. 6.** Schematic configuration of erbium-doped fiber laser pulsed generation.

observed in the C-band region with 1.01 dB transmission loss.

## Laser configuration

Fig. 6 illustrates the ring cavity laser configuration of erbium-doped fiber laser incorporated with CuNWs/PDMS based passive saturable absorber. A 980 nm laser diode (LD) was set up as a pump source in forward pumping configuration. A 2.4 m long erbium-doped fiber (EDF) was pumped through a 980/1550 nm wavelength division multiplexer (WDM) to produce the spontaneous and stimulated emissions at the 1550 nm region. At 980 nm, the absorption of the erbium ions in the EDF is 23 dB/m, whereas its group velocity dispersion (GVD), numerical aperture (NA), and the core and cladding diameters are 27.6 $ps^2$/km, 0.16, 4 μm and 125 μm, respectively. A polarization-insensitive isolator was set in the ring cavity after the EDF to ensure the unidirectional propagation of light oscillating in the laser cavity and to prevent any light reflection, which can devastate the LD. A 90/10 output coupler was used to keep 90% of the oscillating laser light in the cavity, and the remaining 10% of the light was tapped as the output for numerous optical measurements. The SA device was assembled by interposing a small cut of the prepared CuNWs/PDMS based SA between two fiber ferrules with the aid of index matching gel via a fiber connector. The assembled SA was integrated inside the laser cavity as a passive mode-locker. An additional 100 m long single-mode fiber (SMF-28) with a GVD of $-21.7$ $ps^2$/km was also integrated into the cavity to harmonize the dispersion and nonlinearity of the cavity and boost the mode-locking performance. The total net dispersion was calculated to be approximately $-2.25$ $ps^2$/km, and the EDFL cavity works in the anomalous dispersion. The total length of the cavity was approximate with the extended SMF is around 111.4 m The wavelength distribution of the laser output light was observed using an optical spectrum analyser (OSA, Yokogawa AQ6370B), while the temporal analysis was done by a digital oscilloscope (GWINSTEK, GDS-3352), coupled with the photodetector (PD, InGaAs, S145C Integrating sphere Photodiode Power Sensor). A Radio Frequency Spectrum Analyzer (RFSA, Anritsu MS2683 A) was used to measure the radio frequency (RF) power spectrum in conjunction with an integrated PD. The output power was measured by using a power meter (ILX Lightwave OMM-6810B) combined with a power-head (ILX Lightwave OMH-6727B InGaAs).

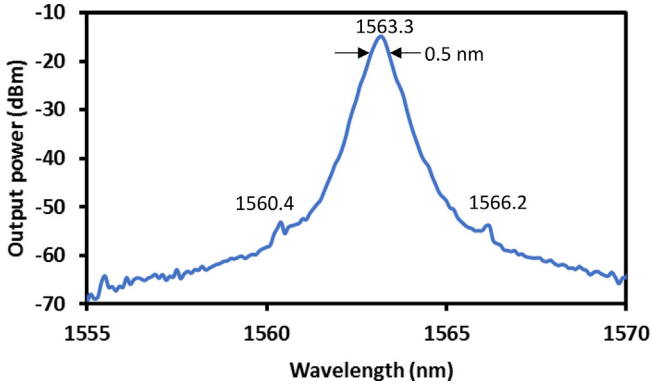


**Fig. 7.** Optical spectrum analyzer trace.

## Results and discussion

The nanosecond mode-locked EDFL self-started at a threshold input pump power of 104.62 mW. The stable nanosecond mode-locking pulses were obtained without any Q-switching pulse fluctuations. The optical spectrum of the laser output is displayed in Fig. 7. As shown in the figure, a broad spectrum obtained proved the mode-locking operation of the EDF laser. The central wavelength was recorded at 1563.3 nm with a 3-dB spectral bandwidth of 0.5 nm at the maximum pump power of 187.04 mW with a pair of the low-intensity peak of Kelly sidebands observed at 1560.4 nm and 1566.2 nm with separation distance with a central wavelength of ± 3 nm. The 3-dB spectral bandwidth is broader than [15] with 0.3 nm. The operation of the laser in the mode-locked soliton regime in anomalous dispersion is confirmed with the existence of symmetrical Kelly sidebands [15].

The mode-locking operation of the EDFL was further investigated by monitoring the pulse train, as indicated in Fig. 8. A uniform pulse train was observed with a constant repetition rate of 1.86 MHz with a pulse separation of 537 ns. The repetition rate remained unchanged from the threshold input pump power of 104.62 mW up to the maximum pump power of 187.04 mW due to energy quantization [25], thus confirming the fundamental characteristics of the mode-locking mechanism. The pulse width was measured to be around 173 ns, as depicted in Fig. 8 (c), shorter than other reported works based on ZnO-SA [19] and Silver-SA [26]. Moreover, the recorded repetition rate of 1.86 MHz was confirmed with the measured value based on the total EDFL cavity length of 111.4 m, implying that the pulsed laser was a nanosecond mode-locked laser.

Furthermore, to explore the signal stability of the frequency, we have to verify the frequency domain from the radio frequency spectrum analyzer (RFSA). The RFSA spectrum of the nanosecond mode-locked EDFL is shown in Fig. 9, where the signal-to-noise ratio (SNR) was 61 dB, higher than the previously reported nanosecond soliton pulse by single-walled carbon nanotubes [27], graphene [28,29] and copper oxide[15]. The RFSA spectrum indicated very good stability for the mode-locked pulse at the fundamental frequency of 1.86 MHz with a span of 10 MHz and resolution bandwidth (RBW) of 3 kHz, respectively. By referring several reported papers, the RFSA of mode-locked fiber laser with pulse width in picoseconds (ps) ranges will produce a constant intensity or small intensity modulation for a span of 100 Mhz (18,

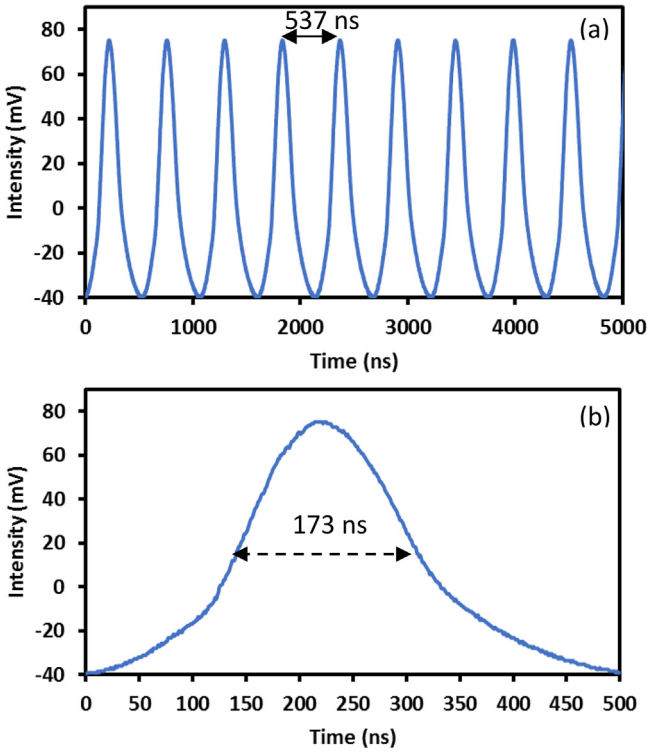


**Fig. 8.** Oscilloscope trace (a) Pulse train (b) single pulse envelope.

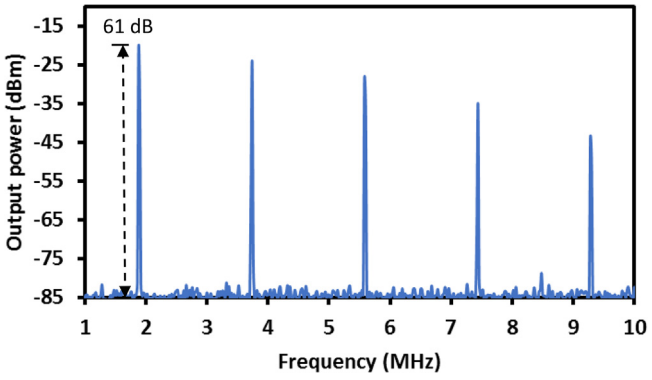


**Fig. 9.** Radio frequency spectrum analyzer trace.

20, 21,22). For nanoseconds mode-locked pulse generation, the pulse width is broader in nanoseconds range and the peak intensity is gradually decreased and maintain at certain peak up to a span of 150 MHz [31] and the same pattern is reported in [19] at span of 7 MHz. By comparing to our recorded Radio frequency spectrum analyser, the pattern is almost the same as reported by [19,31] and it is expected that at a wider frequency span range of RFSA, the peak intensity will gradually decrease until it reaches a constant peak.

Fig. 10 shows the output characteristics of the generated pulses. Fig. 10 (a) shows the output pulse energy and average output power for the nanosecond mode-locked pulses at increasing pump power. As seen, both pulse energy and average output power show an increasing trend against the input pump power. At the maximum input pump power of 187.04 mW, the average output power obtained is 3.41 mW. The pulse energy and instantaneous peak power were calculated at 9.15 nJ, and 6.9 mW, respectively. The peak power linearly increases, from 12.08 mW to 20.66 mW, with the increase in input pump power, as shown in Fig. 10 (b). The stability of the nanosecond mode-locked pulses was monitored under room temperature for one hour. Based on the optical spectrum and pulse amplitude, there was no signal inconsistency

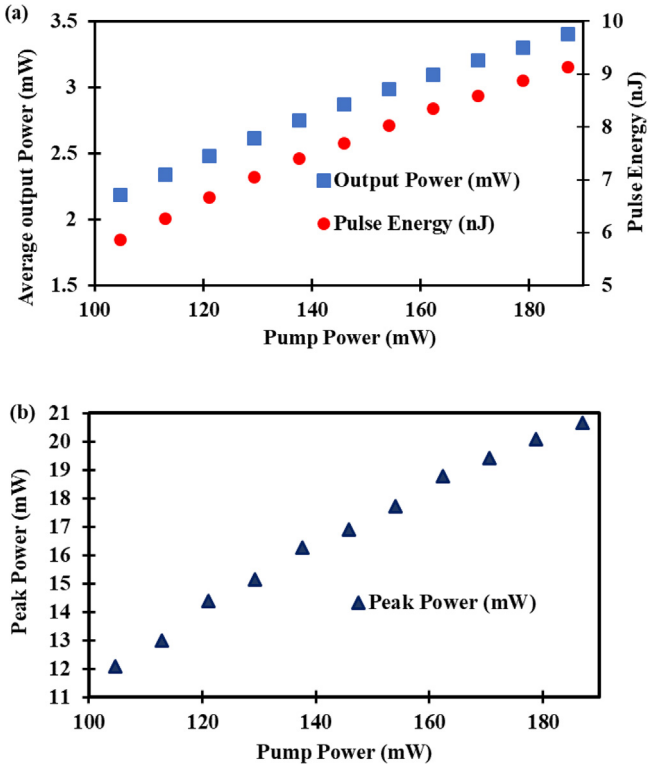


**Fig. 10.** Output characteristics (a) average output power and pulse energy as a function of input pump power, (b) peak power against input pump power.

indicating a good stability of the mode-locked EDFL. In addition, there was no damage to the SA, suggesting that the SA possessed high thermal conductivity property. Table 1 presents the comparison of our work with other SA materials in terms of performance in nanosecond mode-locked EDFL. The pulse energy obtained was higher than those of the carbon-based SAs [272829] and Lutetium (III) oxide [30], and pulse width was shorter than those using SAs made of ZnO [19], silver[26] and SWCNTs [27].

## Conclusion

We have successfully demonstrated a passively self-started and stable nanosecond mode-locked EDFL using CuNWs based SA. The nanosecond mode-locked laser produced had a spectral bandwidth of 0.3 nm and was centred at 1563.3 nm with small Kelly sidebands. The EDFL generated soliton pulses with a fundamental repetition rate of 1.86 MHz and the maximum input pump power of 187.04 mW. The pulse width, pulse energy, and average output power were 173 ns, 9.15 nJ and 3.41 mW, respectively. The metal-based nanowire SA shows an excellent performance in generating nanosecond mode-locked EDF laser.

## CRediT authorship contribution statement

**E.I. Ismail:** Investigation, Validation, Writing - original draft. **F. Ahmad:** Conceptualization, Methodology, Writing - review & editing, Resources, Supervision, Funding acquisition. **S. Shafie:** Writing - review & editing, Resources. **H. Yahaya:** Methodology. **A.A. Latif:** Methodology. **F.D. Muhammad:** Methodology.

## Declaration of Competing Interest

The authors declare that they have no known competing financial interests or personal relationships that could have appeared to

**Table 1**
Previous work for a low repetition rate of mode-locked EDFL with different kinds of SAs.

| SA materials | Repetition rate | Pulse width | Pulse energy (nJ) | Centre wavelength (nm) | References |
|---|---|---|---|---|---|
| SWCNT | 909.1 kHz | 332 ns | 0.34 | 1570.4 | [27] |
| Graphene | 5.78 MHz | 24 ns | 2.10 | 1569.5 | [28] |
| Graphene | 388 kHz | 6 ns | 1.00 | 1560.0 | [29] |
| ZnO | 1 MHz | 400 ns | 11.6 | 1558.3 | [19] |
| Silver | 1.0 MHz | 202 ns | 52.3 | 1561.5 | [26] |
| $Lu_2O_3$ | 0.97 MHz | 2.12 ps | 7.64 | 1564.0 | [30] |
| CuO-PVA | 983 kHz | 1.7 ps | 1.29 | 1564.6 | [15] |
| CuNWs | 1.86 MHz | 173 ns | 9.15 | 1563.3 | This Work |

influence the work reported in this paper.

## Acknowledgements

The authors would like to acknowledge the Universiti Putra Malaysia (9629800) and Universiti Teknologi Malaysia for providing facilities for device fabrication and measurement.

## References

[1] Wang A, Jiang L, Li X, Liu Y, Dong X, Qu L, et al. Mask-free patterning of high-conductivity metal nanowires in open air by spatially modulated femtosecond laser pulses. Adv Mater 2015;27(40):6238–43.
[2] Woodward R, Kelleher E. 2D saturable absorbers for fiber lasers. Applied Sciences 2015;5(4):1440–56.
[3] Guo Bo, Xiao Q-L, Wang S-H, Zhang H. 2D Layered materials: synthesis, nonlinear optical properties, and device applications. Laser Photonics Rev 2019;13(12):1800327.
[4] Ahmad H, Ruslan NE, Ismail MA, Ali ZA, Reduan SA, Lee CSJ, et al. Silver nanoparticle-film based saturable absorber for passively Q-switched erbium-doped fiber laser (EDFL) in ring cavity configuration. Laser Phys 2016;26(9):095103.
[5] Fan D, Mou C, Bai X, Wang S, Chen N, Zeng X. Passively Q-switched erbium-doped fiber laser using evanescent field interaction with gold-nanosphere based saturable absorber. Opt Express 2014;22(15):18537–42.
[6] Muhammad AR, Rosol AHA, Tahrin RAA, Azman NS, Kassim S, Ismail MA, et al. Passive Q-switching operation of erbium-doped fiber laser with gold nanoparticles embedded into PVA film as saturable absorber. Dig J Nanomater Biostruct (DJNB) 2019;14(1).
[7] Guo H, Feng M, Song F, Li H, Ren A, Wei X, et al. Q-switched erbium-doped fiber laser based on silver nanoparticles as a saturable absorber. IEEE Photonics Technol Lett 2015;28(2):135–8.
[8] Ahmad MT, Muhammad AR, Zakaria R, Rahim HRA, Hamdan KS, Yusof HHM, et al. Gold nanoparticle-based saturable absorber for Q-switching in 1.5 μm laser application. Laser Phys 2017;27(11):115101.
[9] Lokman MQ, Yusoff SFAZ, Ahmad F, Zakaria R, Yahaya H, Shafie S, et al. Deposition of silver nanoparticles on polyvinyl alcohol film using electron beam evaporation and its application as a passive saturable absorber. Results Phys 2018;11:232–6.
[10] Muhammad AR, Ahmad MT, Zakaria R, Rahim .RA, Yusoff SFAZ, Hamdan KS, et al., pulse operation in 1.5-μm region using copper nanoparticles as saturable absorber CHIN. PHYS. LETT. 34 3; 2017. Q-switching 034205.
[11] Muhammad AR, Yasin M, Ahmad MT, Zakaria R, Rahim HRA, Jusoh Z, et al. All-fiber ytterbium-doped Q-switched fiber laser based on copper nanoparticle's saturable absorber. Dig J Nanomater Biostruct 2018;13(1):279–84.
[12] Muhammad AR, Ahmad MT, Zakaria R, Yupapin PP, Harun SW, Yasin M. Mode-locked thulium-doped fiber laser with copper thin film saturable absorber. J Mod Opt 2019;66(13):1381–5.
[13] Ismail EI, Ahmad F, Ambran S, Latiff AA, Harun SW, Copper nanoparticles-chitosan based saturable absorber in passively Q-switched erbium-doped fiber laser, AIP Conference Proceedings 2203, 020004; 2020. https://doi.org/10.1063/1.5142096.
[14] Ismail EI, Ahmad F, Ambran S, Latiff AA, Harun SW. Q-switched erbium-doped fiber lasers based on copper nanoparticles saturable absorber. J Phys: Conf Ser 2019;1371:012028https://doi.org/10.1088/1742-6596/1371/1/012028.
[15] Sadeq SA, Harun SW, Al-Janabi AA. Ultrashort pulse generation with an erbium-doped fiber laser ring cavity based on a copper oxide saturable absorber. Appl Opt 2018;57(18):5180–5.
[16] Wu D, Lin H, Cai Z, Peng J, Cheng Y, Weng J, Xu H. Saturable absorption of copper nanowires in visible regions for short-pulse generation. IEEE Photonics J. 2016;8(4):1–7.
[17] Woodward RI. Dispersion engineering of mode-locked fibre lasers. J. Opt. 2018;20(3):033002.
[18] Cui Y, Lu F, Liu X. $MoS_2$-clad microfibre laser delivering conventional, dispersion managed and dissipative solitons. Sci Rep 2016;6: 30524:8.
[19] Alani I, Ahmad BA, Ahmed MHM, Latiff AA, Al-Masoodi AHH, Lokman MQ, et al. Nanosecond mode-locked erbium-doped fiber laser based on zinc oxide thin film saturable absorber. Indian J Phys 2019;93(1):93–9.
[20] Yusoff RAM, Jafry AAA, Kasim N, Zulkipli NF, Samsamnun FSM, Yasin M, et al. Q-switched and mode-locked erbium-doped fiber laser using gadolinium oxide as saturable absorber. Opt Fiber Technol 2020;57:102209.
[21] Rahman MFA, Latiff AA, Rosol AHA, Dimyati K, Wang P, Harun SW. Ultrashort pulse soliton fiber laser generation with integration of antimony film saturable absorber. J Lightwave Technol 2018;36(16):3522–7.
[22] Guo Q, Pan J, Li D, Shen Y, Han X, Gao J, Man B, Zhang H, Jiang S. Versatile mode-locked operations in an Er-doped fiber laser with a film-type indium tin oxide saturable absorber nanomaterials; 2019 9, 701: 11.
[23] Aegerter MA, Mennig M. Sol-gel technologies for glass producers and users. Springer Science & Business Media; 2013.
[24] Zhang B, Li W, Yang Y, Chen C, Li CF, Suganuma K. Fully embedded CuNWs/PDMS conductor with high oxidation resistance and high conductivity for stretchable electronics. J Mater Sci 2019;54(8):6381–92.
[25] Keller U. Recent developments in compact ultrafast lasers. Nature; 2003. 424, (6950): 831.
[26] Rosdin R, Ahmad MT, Muhammad AR, Jusoh Z, Arof H, Harun SW. Nanosecond pulse generation with silver nanoparticle saturable absorber. Chin Phys Lett 2019;36(5):054202.
[27] Ismail MA, Harun SW, Zulkepely NR, Md Nor R, Ahmad F, Ahmad H. Nanosecond soliton pulse generation by mode-locked erbium-doped fiber laser using single-walled carbon-nanotube-based saturable absorber. Appl Opt 2012;51(36):8621–4.
[28] Xu J, Wu S, Liu J, Wang Q, Yang QH, Wang P. Nanosecond-pulsed erbium-doped fiber lasers with graphene saturable absorber. Opt Commun 2012;285(21–22):4466–9.
[29] Xia H, Li H, Wang Z, Che Y, Zhang X, Tang X, et al. Nanosecond pulse generation in a graphene mode-locked erbium-doped fiber laser. Opt Commun 2014;330:147–50.
[30] Baharom M, Rahman MFA, Latiff AA, Wang P, Harun SW. Lutetium (III) oxide film as passive mode locker device for erbium-doped fibre laser cavity. Opt Commun 2019;446:51–5.
[31] Samsamnun FSM, Zulkipli NF, Khudus MIMA, Bakar ASA, Majid WHA, Harun SW. Nanosecond pulse generation with a gallium nitride saturable absorber. OSA Continuum 2019;2(1):134–41.